CONF-880606--3

DE88 011973

3

Thermal Conductivity and Thermal Expansion of Stainless Steels D9 and HT9*

L. Leibowitz and R. A. Blomquist

Argonne National Laboratory, Chemical Technology Division, 9700 S. Cass Avenue, Argonne IL 60439 USA

Abstract: Renewed interest in the use of metallic fuels in liquid-metal fast breeder reactors has prompted study of the thermodynamic and transport properties of its materials. Two stainless steels are of particular interest because of their good performance under irradiation. These are D9, an austenitic steel, and HT9, a ferritic steel. Thermal conductivity and thermal expansion data for these alloys are of particular interest in assessing in-reactor behavior. Because literature data were inadequate, measurements of these two properties for the two steels were performed and are reported to 1200 K. Of particular interest is the influence on these properties of a phase transition in HT9.

1. Introduction

Recently increased interest in metallic fuels for liquid-metal fast breeder reactors [1] has prompted a reassessment of the available thermodynamic and transport property data for the materials of interest. The two primary cladding alloys under consideration are the stainless steels D9, an austenitic alloy, and HT9, a ferritic steel.

Modeling of fuel performance and reactor behavior depend, in part, on the thermodynamic and transport properties of the cladding. Because of a lack of reliable data for D9 and HT9, we undertook measurements of their thermal expansion and thermal conductivity. Our results are reported below.

2. Experimental

2.1 Materials

The cladding alloys studied were D9, an austenitic steel similar to 316 stainless steel, and HT9, a ferritic alloy, similar to 400 series steels. The compositions are, for D9, 15.5 wt % Ni, 13.5 wt % Cr, 2.0 wt % Mn, 2.0 wt % Mo, 0.75 wt % Si, 0.25 wt % Ti and 0.04 wt % C, and for HT9, 0.5 wt % Ni, 12.0 wt % Cr, 0.2 wt % Mn, 1.0 wt % Mo, 0.25 wt % Si, 0.5 wt % W, 0.5 wt % V and 0.2 wt % C, with the balance Fe. The alloys were used in the as-received condition. The D9 was solution annealed at 1322 K and 20% cold worked; the

*This work supported by the U. S. Department of Energy

DISCLAIMER

HT9, which had a martensitic structure, was tempered by heat treating at 1311 K and at 1033 K.

2.2 Thermal Expansion

Thermal expansion measurements were performed using a Netzsch Inc. Model 402 dilatometer. This is a horizontal, single push rod dilatometer with a rhodium furnace. The instrument has also been installed in the helium-atmosphere glove box and it is connected to a CAMAC Inc. data acquisition system which is interfaced to a Digital Equipment Corp. (DEC) PDP-11/34 computer. The sample is held in an alumina support tube, closed at one end, and is located in the center of the constant temperature zone of the furnace. A vacuum-tight protective tube allows control of the atmosphere to which the sample is exposed. An alumina rod in a frictionless support transfers the change in length of the sample to an inductive displacement transducer. Sample temperatures are measured with a Type S (Pt vs Pt-10% Rh) thermocouple.

In a typical measurement, a 50 mm long sample, prepared with flat, parallel end faces, was installed in the instrument. The furnace was evacuated and flushed with high purity helium several times and finally filled with high purity helium to a pressure slightly above ambient. The desired set of temperature cycles was entered in the controller and the test series begun. The dilatometer was periodically calibrated with an NBS tungsten thermal expansion standard (SRM 737). A variety of heating and cooling rates were tested and 1 K per minute was chosen as the standard rate. As will be discussed below, complications caused by phase changes in HT9 led to tests at lower rates. For the NBS standard and D9, however, 1 K/min was satisfactory. Length changes measured with the dilatometer depend on the differences between expansion of the sample and its holder. From the known thermal expansion of the NBS standard, a correction due to expansion of the sample holder was calculated and applied to subsequent measurements. Separate temperature calibrations were performed using NBS aluminum (SRM 44f) and high purity gold (reported to be 99.99 % pure). These calibrations were performed by using a foil of the metal between two 25.4

mm long alumina rods in place of the normal thermal expansion sample. The temperature at which a sharp change in length was observed was taken as the melting point of the metal. In all cases our indicated temperatures were within ±2 K of the expected melting point. We estimate the accuracy of our thermal expansion data to be about ±2% although the precision is significantly better.

2.3 Thermal Conductivity

Thermal conductivity measurements were performed using a Dynatech Corp. Model TCFCM–N20 thermal conductivity instrument. Because it is being used for measurements on plutonium–containing materials, the instrument is located in a helium–atmosphere glove box. The hot zone of the instrument is further protected from gaseous impurities by enclosing it in a large aluminum bell jar, secured to the base plate through a rubber gasket. The bell jar can be evacuated and filled with high–purity helium. The apparatus is based on the comparative thermal conductivity method [2]. An unknown cylindrical sample is positioned under spring tension between two identical, calibrated reference cylinders, thereby forming a vertically stacked column. Longitudinal heat flow is established by heaters placed above and below the column. The bottom heater rests on a water-cooled block and serves as a heat sink. Radial heat losses are minimized by surrounding the column with guard furnaces in which the thermal gradient is matched to that of the column and by filling the annular space with foamed-yttria granules.* Foamed–yttria was used because of its good compatibility with the uranium–plutonium–zirconium alloys also being studied and because it lessened problems of dust within the glove box.

Six ungrounded chromel-alumel thermocouples sheathed in Inconel were used for temperature measurements. Each of the three cylinders comprising the experimental stack held two thermocouples in wells a known distance apart No thermocouple calibrations were made because only the differences in temperature were of consequence in calculating thermal con-

*The foamed yttria was prepared for us by R. B. Poeppel (Argonne National Laboratory).

ductivities and because all thermocouples were derived from the same batch. In earlier work with this instrument, thermocouple calibrations were performed and found to be negligible.

In a typical experiment, the column was assembled and the thermocouples were inserted into their designated wells. After lowering the guard furnace, the annular space was filled with yttria granules and covered with quartz wool. After the bell jar had been lowered on the base plate, the assembly was evacuated, degassed for several hours at 300°C, flushed several times with ultra-high purity helium, and then backfilled with helium to a pressure of ~80 kPa. The top and bottom heaters were programmed for the desired temperature gradient (~ 80 K) and the system allowed to come to steady state. At the end of equilibration, thermocouple outputs were measured with a digital voltmeter to within $\pm 5\mu$V, and the heaters were re-programmed for the next temperature.

Our experience has indicated that slight heat flux (q_i) differences, noticeable between the top and bottom references, are functions of the total temperature gradient (ΔT) imposed on the column between the top and bottom thermocouples. In earlier measurements, we attempted to improve the accuracy of our data by obtaining at least two values of ΔT selected in such a way that the condition $q_{top} > q_{bottom}$ existed at the lower ΔT value and $q_{top} < q_{bottom}$ at the higher value. Linear interpolations (or in some cases extrapolations) were then used to establish a value of ΔT at which there was an identical heat flux (q_{ref}) in both references and also to determine the corresponding average value of the sample temperature centered between the thermocouples in the unknown. Thermal conductivity of an unknown sample is then calculated from the following equation:

$$\lambda_{sample} = \left(\frac{\Delta x}{\Delta T}\right)_{sample} \left(\lambda \frac{\Delta T}{\Delta x}\right)_{ref} \qquad (1)$$

Subsequent measurements shoed that no significant difference in reliability was obtained by using this procedure. In the work described here, only a single gradient was used at which differences in heat fluxes in the top and bottom references were insignificant.

The primary thermal conductivity reference standard used in this study was austenitic stainless steel (SRM 1462) supplied by the National Bureau of Standards (NBS). Its chemical composition was given as 62.0 wt % Fe, 20.2 wt % Ni, 16.2 wt % Cr, 1.2 wt % Mn, 0.28 wt % Si, and <0.01 wt % C.

Cylindrical Samples about 25.4 mm in diameter and 25.4 mm high were machined from available stock and thermocouple wells 12.7 mm long and 1.7 mm in diameter were drilled 6.35 mm from the top and bottom of each sample. The faces of the samples were carefully polished to provide good thermal contact.

Thermal expansion corrections were made to the interwell distances of all alloys used. Our own thermal expansion values were used for the cladding alloys D9 and HT9. For the NBS reference, data were taken from the compilation by Touloukian et al.[3], substituting Fe + (24–26) w/o Ni + (15–20) w/o Cr + Σx_i for the NBS standard. Thermal expansion corrections between room temperature and 1200 K were 1.4% for the NBS reference, 1.8% for D9 and 1.1% for HT9.

Test measurements were performed in which all three cylinders were NBS reference steel, that is we measured the thermal conductivity of the NBS standard in the same way we would measure our unknown alloys. These measurements were within the stated uncertainty of the NBS of 5%. We estimate the accuracy of our measurements on cladding alloys to be about ±10% although, as will be discussed below in connection with phase transitions in HT9, the precision is significantly better.

3. Results

3.1 Thermal Expansion

D9: Thermal expansion data for D9 are shown in Fig. 1 and compared in that figure with data for 316 stainless steel of similar composition reported by Lucks et al. [4] and with values given by Touloukian et al. for 300 series stainless steels, including 316. No data are available in the literature for the thermal expansion of D9. The composition of the steel used by Lucks et al. [4] was, 11.6 wt % Ni, 16.82 wt % Cr, 1.59 wt % Mn, 2.18 wt % Mo, 0.26 wt % Si, 0.103

wt % C, 0.023 wt % S, and 0.018 wt % P, with the balance Fe. One point tabulated at 850°C in Ref. 4, which appears to have been a typographical error, was omitted from the plot. As can be seen in Fig. 1, the agreement between the three sets of data is good and, in contrast with HT9 as will be discussed below, no phase transitions are apparent. The key features of present interest in these steel alloys are the existence of an fcc γ–phase (austenite) and a bcc α–phase (ferrite). From an inspection of the Fe–Cr–Ni phase diagram [5], no transitions from the γ–phase would be expected in D9. Heating and cooling cycles agreed very well for this alloy. The pooled results of six heating and cooling cycles at 1 K/min are described by Equation 2 with a percent standard deviation (σ) of 0.17. In that equation, and others for thermal expansion, the temperature, T, is in K, and the relative change in length referenced to 293 K is given in percent. That is $\Delta L/L_0 = 100 \times [L(T) - L(293)]/L(293)$

$$\Delta L/L_0 = -0.4247 + 1.282 \times 10^{-3}T + 7.362 \times 10^{-7}T^2 - 2.069 \times 10^{-10}T^3 \qquad (2)$$

HT9: Thermal expansion data for HT9 are shown in Fig. 2. It is evident that in this case an obvious transition is occurring at about 1050 K. Inspection of the Fe–Cr phase diagram [6] and the Fe–Cr–Ni diagrams [5] shows that shows that a $\alpha \rightarrow \gamma$ transition would be expected at roughly that temperature. On cooling, however, the transition is substantially delayed even at 1 K/min. In commenting on the Fe–Cr–Ni phase diagram in Ref. 6 it is noted that "The outstanding feature, however, is the pronounced reluctance of metastable austenite to transform when once established at high temperatures." The hysteresis shown in Fig. 2 clearly demonstrates this effect. Also shown in Fig. 2 are data for the thermal expansion of HT9 taken from an industrial data sheet [7] and from values given by Touloukian et al. for 400 series stainless steels, including 410, similar to HT9. Although Ref. 7 is not a very satisfying source, the agreement of Refs. 7 and 3 with our results the lower temperatures is remarkably good. Equation 3 ($\sigma = 0.17$) represents the heating–cycle data up to about 1050 K.

$$\Delta L/L_0 = -0.2191 + 5.678 \times 10^{-4}T + 8.111 \times 10^{-7}T^2 - 2.576 \times 10^{-10}T^3 \qquad (3)$$

This equation may be used for both heating and cooling cycles provided the transition temperature is not exceeded.

It was not feasable for us to perform thermal expansion measurements at lower heating rates than 1K/min. It appears that the transition observed does not occur at the equilibrium temperature even at that low heating rate. Results of thermal conductivity measurements (see below), which we believe do represent equilibrium, show a transition at about 1050 K, in better agreement with expectations from the phase diagrams.

3.2 Thermal Conductivity

D9: In the absence of literature values for the thermal conductivity of D9, our measured thermal conductivity data for D9 are compared in Fig. 3 with literature values for 316 stainless steel [4,8,9]. As can be seen agreement is quite good with the data of Lucks et al. [4] but, at the higher temperatures, not as well with the data of Matolich [8] or of Chu and Ho. The composition of Matolich's sample of 316 stainless steel whose data are shown in Fig. 3 (his designation 3A) was, 12.60 wt % Ni, 17.45 wt % Cr, 1.59 wt % Mn, 2.55 wt % Mo, 0.6 wt % Si, 0.063 wt % C, 0.01 wt % S, 0.023 wt % P, 0.09 wt % Cu, and 0.19 wt % Co, with the balance Fe. The values of Chu and Ho arose from an assessment of a great many measurements on 316 stainless steel. It is difficult to account for the differences shown by the values in Fig. 3, which, considering the accuracy of these measurement, are of marginal significance.

Our data for D9 were taken in random temperature order to minimize any influence of instrument drift or other sources of systematic error. There seems to be a change in the our data at about 1000 K and we have represented the values to 1000 K by equation 4 ($\sigma = 0.47$)and values above 1027 K by equation 5 ($\sigma = 0.51$).

$$\lambda = 7.598 + 2.391 \times 10^{-2}T - 8.899 \times 10^{-6}T^2 \quad (4)$$

$$\lambda = 7.260 + 1.509 \times 10^{-2}T \quad (5)$$

The thermal conductivity, λ, is in W/mK and the temperature, T, is in K.

It is difficult to speculate on the cause of the break in these thermal conductivity data in the absence of additional information, but it appears structural. No corresponding features were observed in thermal expansion. The coincidence in transition temperatures with HT9, below, could indicate the presence of a small amount of a ferrite phase, perhaps formed as a consequence of the high temperatures to which this sample was subjected.

HT9: The phase transition shown by HT9 had a profound influence on our thermal conductivity measurements. Our data are shown in Fig. 4 along with values taken from an industrial data sheet for HT9 [7] and the values recommended by Chu and Ho [9] for 410 stainless steel. In the region of overlap, agreement is reasonably good with the smoothed Sandvik [7] values, which, however, are quite sparse. Agreement with the Chu and Ho values is also fairly good considering that they apply to different steels. Chu and Ho comment that there are no data for temperatures above 1000 K and their recommended values above that temperature are based on extrapolations. Our experience with these measurements has shown that it is extremely difficult to obtaining reproducible data much above that temperature. Reproducible values could be obtained in random temperature order either entirely below or entirely above the transition temperature. It was very difficult, however, to move from above to below the transition temperature and reproduce the lower temperature data. This could be done only by changing the temperature in very small steps and waiting for long times. Moving from below to above the transition was much simpler, in accord with expectations of the ferritic–to–austenitic transformation. Equation 6 ($\sigma = 0.57$) below, represents our data below the transition at 1027 K, and equation 7 reproduces the data ($\sigma = 0.30$) above 1050 K.

$$\lambda = 17.622 + 2.428 \times 10^{-2}T - 1.696 \times 10^{-5}T^2 \qquad (6)$$

$$\lambda = 12.027 + 1.218 \times 10^{-2}T \qquad (7)$$

The thermal conductivity, λ, is in W/mK and the temperature, T, is in K.

4. Discussion and Conclusions

Data have been presented for thermal expansion and thermal conductivity of the steel alloys D9 and HT9. The austenitic alloy, D9, is reasonably well behaved and shows values for both thermal expansion and thermal conductivity typical of 316 stainless steel. The ferritic alloy, HT9, however, shows a phase transition in the neighborhood of 1050 K and is similar to 410 stainless steel in these properties. Although 1050 K is far above the recommended service temperature of HT9, assessments of its behavior under severe, unexpected conditions, such as hypothetical nuclear reactor accidents, must take these effects into account.

References

1. Leon C. Walters, B. R. Seidel, and J. Howard Kittel, Nucl. Tech. 65 179 (1984).
2. J. Francl and W. D. Kingery, J. Am. Ceram. Soc., 37 80 (1954).
3. Y. S. Touloukian, R. W. Powell, C. Y. Ho, and P. G. Klemens, "Thermophysical Properties of Matter," Vol.12, Thermal Expansion, IFI/Plenum, New York, 1970.
4. C. F. Lucks, H. B. Thompson, A. R. Smith, F. P. Curry, H. W. Deem, and G. F. Bing, United States Air Force Technical Report, USAF–TR–6145–1, February, 1951.
5. "Metals Handbook", 8th Edition, Vol. 8, Metallography, Structure, and Phase Diagrams, American Society for Metals, Menlo Park, OH, p. 425, 1973.
6. M. Hansen, "Constitution of Binary Alloys," McGraw-Hill, N.Y. 1958.
7. Sandvik data sheet, "SANDVIK HT9" S–1720–ENG, SANDVIK steel catalogue, May, 1981.
8. J. Matolich, Jr. , Battelle Memorial Inst. Report, BATT–7096, Sept. 1965, (also classified as NASA–CR–54151).
9. T. K. Chu and C. Y. Ho, Proc. 15th Int. Conf. on Thermal Conductivity, V. V. Mirkovich, Ed. Plenum, N.Y., 1978, p. 79.

List of Figures

1. Thermal expansion of D9 compared with data of Lucks et al. [4] and Touloukian et

al. [3] (TPRC) for 316 stainless steel.

2. Thermal expansion of HT9 compared with data given for HT9 by SANDVIK [7] and for 410 stainless steel by Touloukian et al. [3] (TPRC); "Heating" and "Cooling" designate data obtained respectively for heating and cooling cycles.
3. Thermal conductivity of D9 compared with data for 316 stainless steel of Matolich [8], Lucks et al. [4], and Chu and Ho [9].
4. Thermal conductivity of HT9 compared with data given for HT9 by SANDVIK [7] and for 410 stainless steel by Chu and Ho [9].

Thermal Expansion, D9

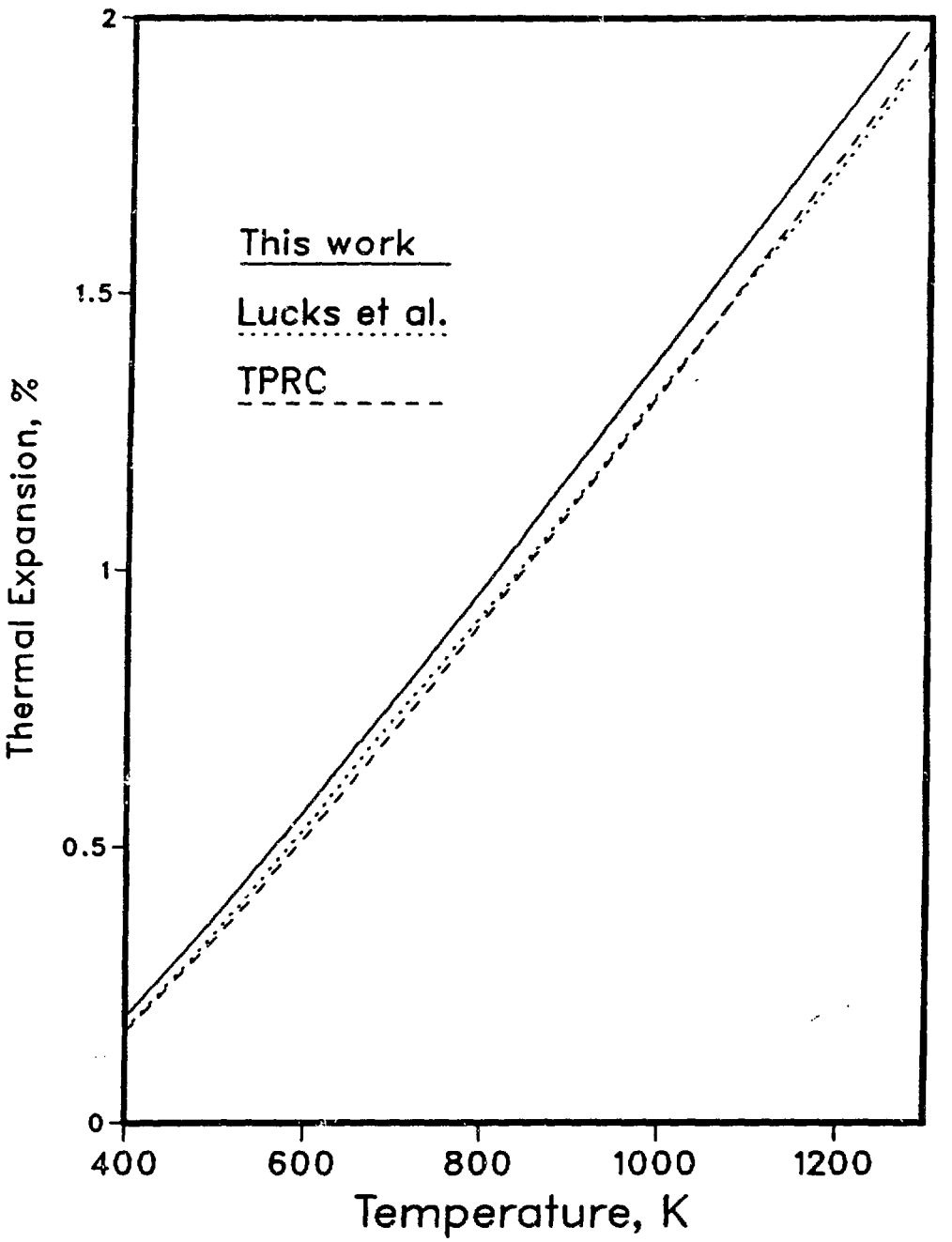

Thermal Expansion, HT9

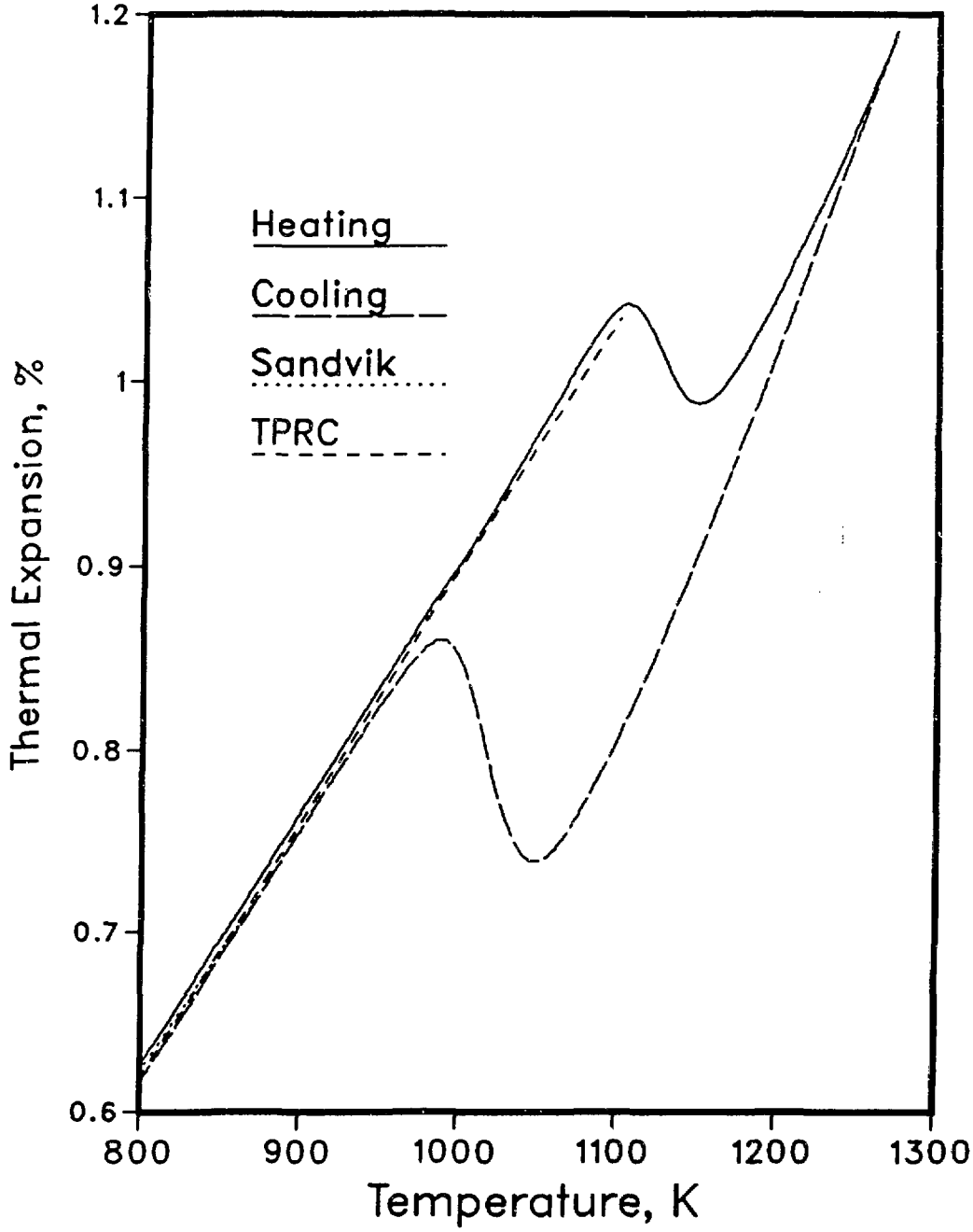

Thermal Conductivity, D9

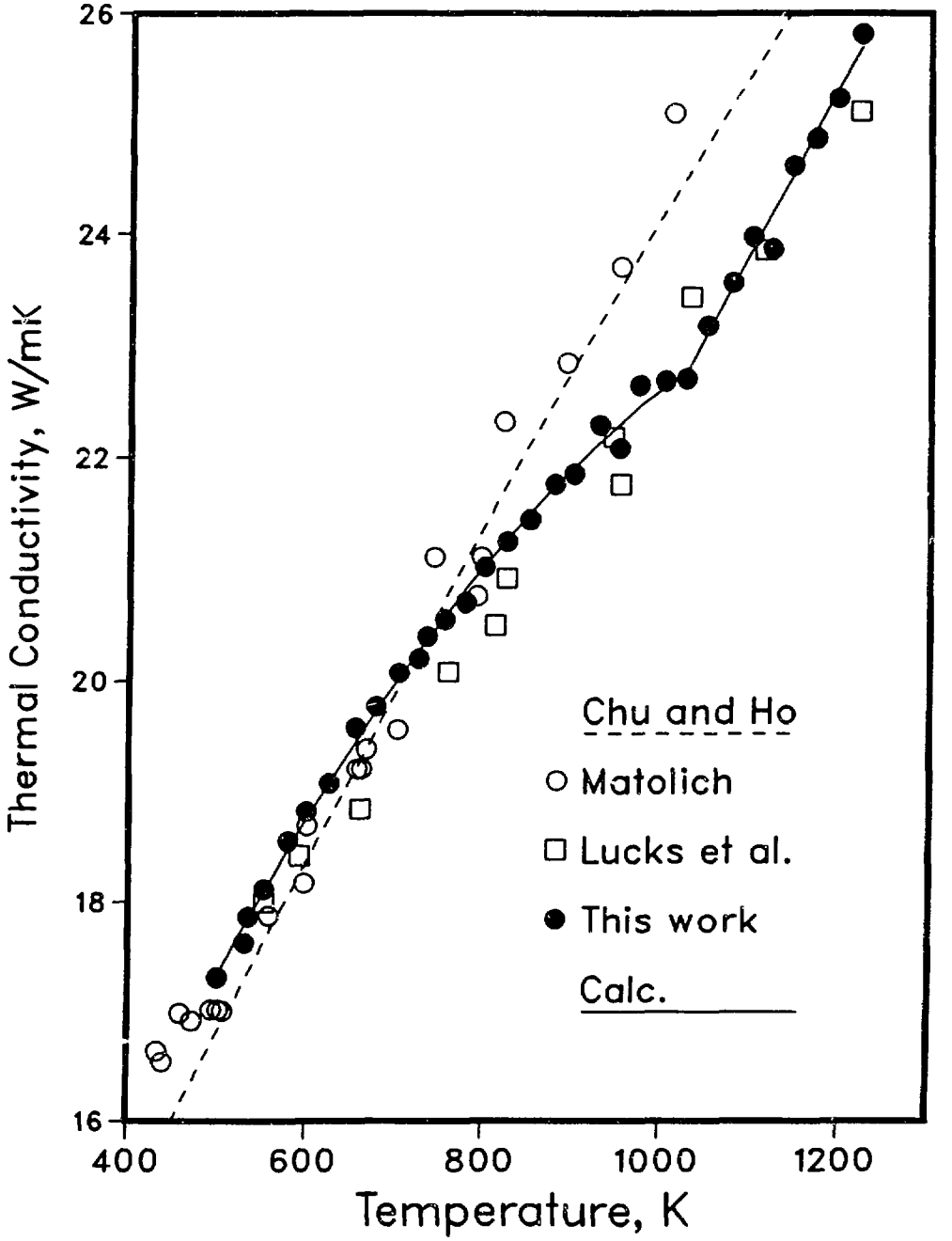

Thermal Conductivity, HT9